Advancements in Ocular Vascularization Analysis Using Deep Learning Techniques – A Systematic Review

F Rahman [1*], Akanksha Mishra [1], Sushree Sasmita Dash [1]

Abstract

In this review, we have investigated the critical examination of ocular vascularization for clinical assessment, specifically in the context of retinopathies associated with systemic disorders. The study emphasizes the impact of high blood pressure and diabetes on the development of hypertensive and diabetic retinopathy, respectively. Traditionally, identifying and classifying blood vessels in medical imaging has been time-consuming and prone to errors. The introduction of Machine Learning (ML), particularly Deep Learning (DL) methods, has revolutionized the process, allowing for more efficient and precise identification and categorization of blood vessels. The research proposes a cutting-edge ML framework utilizing Convolutional Neural Networks (CNNs) and ensemble learning to optimize blood vessel segmentation and classification. The primary goal is to enhance both speed and efficiency, addressing common challenges in processing medical images. The application of these advanced algorithms not only represents a technological achievement but also a significant stride towards personalized and accurate medical care. Our review consolidates existing research findings, compares methodologies, and highlights the progress in ML techniques that have improved the speed and efficacy of blood vessel segmentation, particularly in ophthalmology.

Keywords: Ocular vascularization, Retinopathies, Machine learning in medical imaging, Blood vessel segmentation, Retinal image analysis

Significance | This review shows an advanced machine learning method for efficient segmentation and classification of blood vessels in medical images, revolutionizing diagnostic precision.

*Correspondence. F Rahman, Faculty of CS & IT, Kalinga University, Naya Raipur, Chhattisgarh, India.
E-mail: ku.vijaykumarjaiswal@kalingauniversity.ac.in

Editor Aman Shah Abdul Majid & Md Shamsuddin Sultan Khan And accepted by the Editorial Board Jan 24, 2024 (received for review Nov 15, 2023)

1. Introduction

An examination of ocular vascularization is a crucial aspect of the clinical assessment of systemic disorders that result in the abnormal development or distortion of BVs in the retina (retinopathies). High blood pressure can lead to hypertensive retinopathy, characterized by increased vessel tortuosity, vascular reflex anomalies, and the development of new BVs or neovascularization Triwijoyo et al. (2020). Diabetes can cause diabetic retinopathy, which involves weakening and alterations of retinal vessels, resulting in microaneurysms and haemorrhages in early stages and abnormal BV growth in advanced stages Kim et al. (2023).

The retina is the ocular receptive layer that is accountable for visual perception. The key structural elements it comprises are the Optic Disc (OD), the macula, and the BVs. The ocular converge towards the center of the OD and extend over the entire cornea, excluding the macula, while undergoing a decrease in width. Various eye diseases change the shape of the blood vessels in the

Author Affiliation.
[1] Faculty of CS & IT, Kalinga University, Naya Raipur, Chhattisgarh, India.

Please cite this article.
F Rahman, Akanksha Mishra, Sushree Sasmita Dash, (2024). Advancements in Ocular Vascularization Analysis Using Deep Learning Techniques – A Systematic Review, Journal of Angiotherapy, 8(1), 1-9, 9487

eye Boudegga et al. (2021). The generative phase of Diabetic Retinopathy (DR), also known as the damp state of Developmental Macular Generation (DMD), involves the formation of new BVs that are thinner, distorted in shape, and have less contrast compared to the existing BVs Krestanova et al. (2020). In the non-invasive phase of DR and cardiovascular retinopathy, the leaking of BVs leads to the development of many lesions along the vascular network, such as micro-aneurysms. The retinal BV tree is regarded as a primary indicator for various ocular disorders. The assessment and classification of these disorders have traditionally relied on changes in the structure of the BVs Mookiah et al. (2021).

Traditionally, the task of identifying and separating BVs in medical imaging, especially in retinal scans, has been time-consuming and susceptible to mistakes made by humans, resulting in uneven and untrustworthy outcomes Zhou et al. (2021). The introduction of ML, namely DL methods, has brought about a dramatic transformation in the processing and interpretation of these pictures. Algorithms have been created that can not only equal, but often exceed individual precision in detecting and categorizing blood arteries in different medical pictures. This advancement represents not only a technical feat but also a significant therapeutic breakthrough, providing the possibility of early identification and intervention in conditions such as DR, cataracts, and diverse cardiovascular illnesses (Naramala et al. 2023, Rutba-Aman et al., 2023, Tanvir et al., 2023).

This research aims to provide a framework that utilizes cutting-edge ML techniques to accurately segment and classify blood arteries Imran et al. (2019). The primary objective of this system is to achieve optimal speed and efficiency by targeting the typical obstacles encountered in processing medical images, such as substantial computing expenses and prolonged processing durations. Through the optimization of the algorithm to enhance both efficiency and precision, the framework may be effortlessly incorporated into clinical processes, offering healthcare practitioners real-time help Zhao et al. (2019).

In addition, the research investigates the use of sophisticated ML techniques, such as CNNs and ensemble learning approaches, to improve the precision and dependability of BV segmentation Bhatia et al. (2022). The use of these advanced algorithms is not only a technological undertaking, but rather a progression towards tailored and accurate medical care. This technique enables the creation of precise and comprehensive maps of a patient's blood vessels, hence enabling the development of customized treatment strategies and enhancing patient results.

Concisely, this study introduces a state-of-the-art method for analyzing medical images. The suggested ML architecture has the potential to optimize the procedure of BV segmentation and categorization, as well as to provide new opportunities for early identification and management of vascular illnesses Islam et al. (2021). The incorporation of ML into medical imaging is a crucial point in the convergence of technology and healthcare, with the possibility to significantly improve treatment of patients.

2. Related works

The use of ML in evaluating medical images, namely in the segmentation and categorization of BVs, represents notable progress in diagnostic techniques. Jiang et al. (2019) devised a technique for segmenting retinal BVs using CNN Jiang et al. (2019). When applied to a particular database of retinal images, this approach produced an accuracy rate of 95.4%, a sensitivity rate of 76.2%, and a specificity rate of 97.8%.

Siddiqi et al. (2021) used ML methodologies to separate and classify cardiac angiographic pictures. The model demonstrated a comprehensive accuracy of 92% in categorizing various cardiac diseases Siddiqi et al. (2021). This approach integrates the fields of image processing and ML, offering a valuable tool for the timely detection and planned implementation of treatments in cardiology. The drawback encompasses the possible difficulties in handling angiographic pictures of poor quality and the intricacy of using the technology in various clinical environments.

In their study, Dang et al. (2022) presented Vessel-CAPTCHA, a learning system designed to annotate and segment vessels in medical pictures Dang et al. (2022). It exhibited a vascular segmentation accuracy of 89% applied to diverse medical picture datasets. The framework's efficacy and precision render it appropriate for medical use, notwithstanding potential difficulties in managing low-contrast or high-noise pictures.

Islam et al. (2021) introduced a DL approach to diagnose glaucoma, explicitly focusing on segmenting the optic cup, optical disc, and BVs Islam et al. (2021). The use of the algorithm on retinal pictures demonstrated a detection accuracy of 87.5%. The focused methodology is beneficial for identifying glaucoma, but its efficacy for other retinal disorders may be limited owing to its specialized character.

In their study, Gegundez-Arias et al. (2021) devised a DL technique to segment BVs in retinal pictures. They achieved an impressive accuracy of 94%, a sensitivity of 71%, and a specificity of 98% by using convolutional kernels and a modified U-Net model. The method's superior capability in accurately dividing delicate BVs is beneficial, yet it may encounter challenges when dealing with pictures of diverse quality Gegundez-Arias et al. (2021).

In their study, Kumar and Singh (2023) investigated using a combination of advanced ML models to predict retinal diseases. Specifically, they focused on segmenting and classifying BVs in the retina. Their approach included integrating several neural network topologies to improve the precision and resilience of segmentation

(Kumar, Singh, 2023). Upon implementation, this technique demonstrated a segmentation accuracy of 96% and a disease prediction accuracy of 93%.

In their study, Zhao et al. (2019) performed a thorough examination that compared rule-based and ML-based techniques for segmenting BVs Zhao et al. (2019). They emphasized many methods, each showcasing distinct performance indicators on diverse datasets. For example, some ML models achieved up to 94% accuracy, but the performance of rule-based approaches varied greatly depending on the specific rules used. The primary benefit of ML techniques is their inherent flexibility and capacity to learn, often achieving superior accuracy levels.

Boudegga et al. (2021) devised a rapid and effective technique for segmenting retinal BVs using DL networks Boudegga et al. (2021). Their suggested model successfully attained a remarkable accuracy of 95% in the segmentation of retinal BVs while also exhibiting a reduced processing time compared to conventional approaches. The efficacy of this approach is in its rapidity and precision, making it appropriate for medical applications requiring real-time processing. However, the caliber of the training data greatly influences the model's effectiveness, and it may encounter difficulties when presented with pictures that substantially differ from the training set concerning quality or attributes Dang et al. (2022).

This survey aims to consolidate existing research outcomes, compare techniques, and emphasize the progress made in ML methods that have improved the quickness and efficacy of BV segmentation Moccia et al. (2018). This improvement has resulted in more precise and prompt diagnoses in ophthalmology and other healthcare disciplines.

3. Proposed method

This paper presents a technology that mainly utilizes a fully CNN to segment vascular components in the initial color retinal pictures. This technique is defined by many essential elements:

Network Architecture: It refers to the design and structure of a computer network, including its components, connections, and protocols. The research presents a clearly defined network structure, highlighting the improvements and modifications made to the RU-Net model. This model serves as the fundamental framework, providing guidance for the structural design of the network.

Phase of Learning: Essential to the process is the training phase, which encompasses a sequence of phases. These tasks include acquiring the required data, creating input-output pairings for the network, and identifying the most appropriate loss function and parameters to efficiently train the network.

Utilization of the trained neural network: After the training phase, the attention turns to the implementation of this trained network. During this phase, the network is implemented for real-world inference tasks, resulting in the generation of binary BV pictures Samuel et al. (2021). Translating the theoretical components of the network into feasible, practical use is a critical step.

The system structure utilized in this study is derived from the RU-Net networking framework but has been altered from its original design. The network complexity has decreased from 4 to 3, resulting in the input picture being reduced to 16 x 16 before the upscale stage begins. The convolutions used in every layer have been substantially decreased from a series of [32, 64, 128, 256, 512] CONV in the initial network to a consistent series of [16, 16, 16, 16] convolutions. This alteration, in conjunction with the prior one, significantly affects the parameters that need to be calibrated in the network. The user's text consists of a bullet point symbol. RB has been included in the downsizing and scaling-up stages while using BN Balasubramanian et al. (2021).

Fig. 1 describes the proposed RU-Net for segmentation of retinal BVs. The subsequent blocks have been identified: The CONV_ReLU block is a component that combines a convolutional layer with a rectified linear unit activation function. This block performs a convolution operation on the input using a 3 × 3 kernel and the stride quantity as an optional parameter. The Rectified Linear Unit (ReLU) activation parameter processes the convolution output. The BN_RELU_CONV block is a component that applies batch normalization, ReLU activation, and convolution operations. This block performs batch normalization on the input, applies the ReLU activation function, and finally performs a convolution process using a 3 × 3 kernel and a stride number of 1.

The BN_RELU_CONV(2) block is applied after the BN_RELU_CONV block twice in a sequential manner.

Block 1: This operational block is used in the downsampling pathway. The process involves the consecutive application of a Conv ReLU block, followed by two BN_RELU_Conv_2 blocks. Each BN_RELU_Conv_2 block is equipped with a bypass connection.

Block 2: This operational block is used in increased sampling. The input of this block consists of the output from the preceding block and the list of features created at the identical deeper level in the down-sampling route. An inverted convolution with a 3 × 3 kernel and a step value of 3 is used to resize the output of the preceding block to match the dimension of the input feature mapping. The outcome of the preceding procedure is connected to the feature map provided to generate a unified feature map.

The freshly added feature map undergoes processing in a Conv_ReLU block, followed by a BN_RELU_Conv_2 block incorporating the bypass connection. The network input has been optimized to process sub-images of 128 × 128 pixels rather than the whole fundus picture. The primary benefit of using smaller

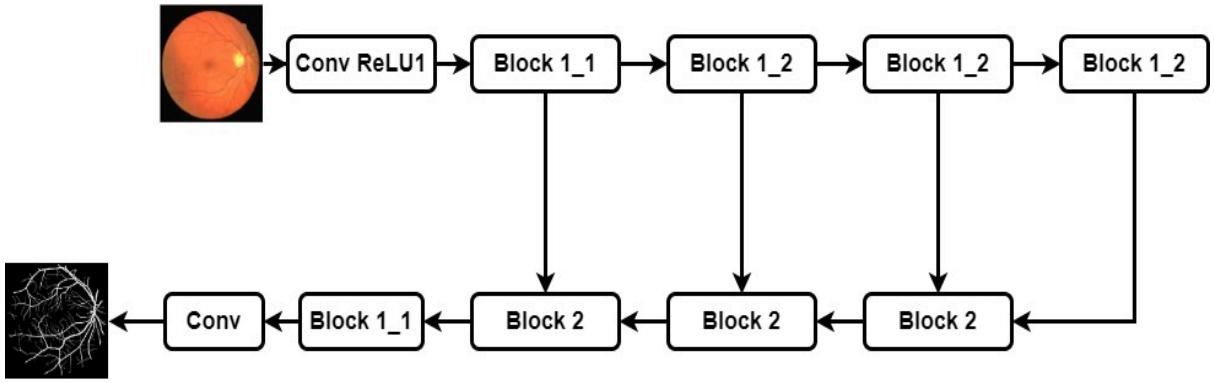

Figure 1. Architecture of the proposed RU-Net for segmentation of retinal BV

Figure 2. An exemplification of the data source used during the learning stage

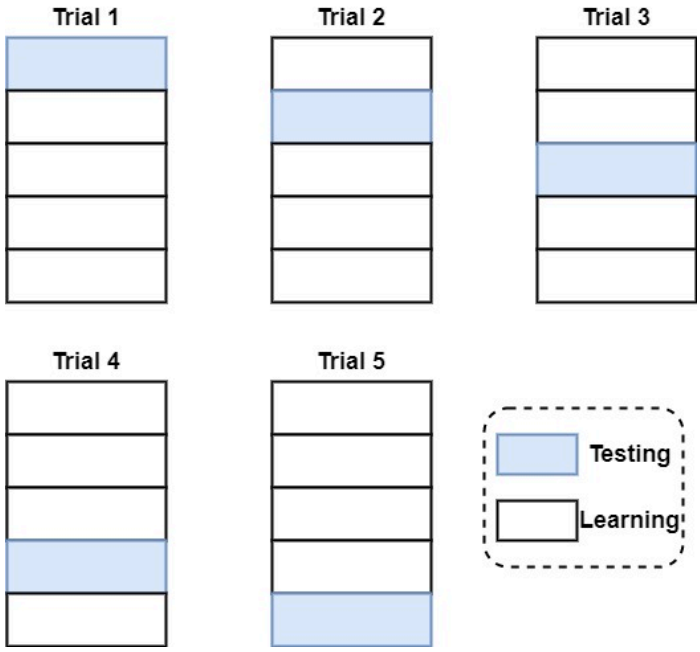

Figure 3. Allocation of segments for learning and testing using a five-fold cross-verification technique.

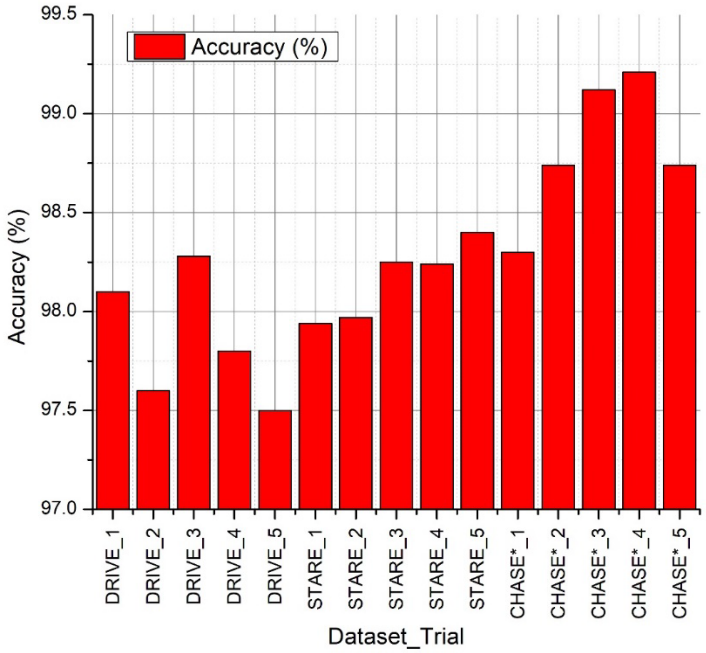

Figure 4. Accuracy (%) of RU-Net segmentation process using a five-fold cross-verification technique for various datasets.

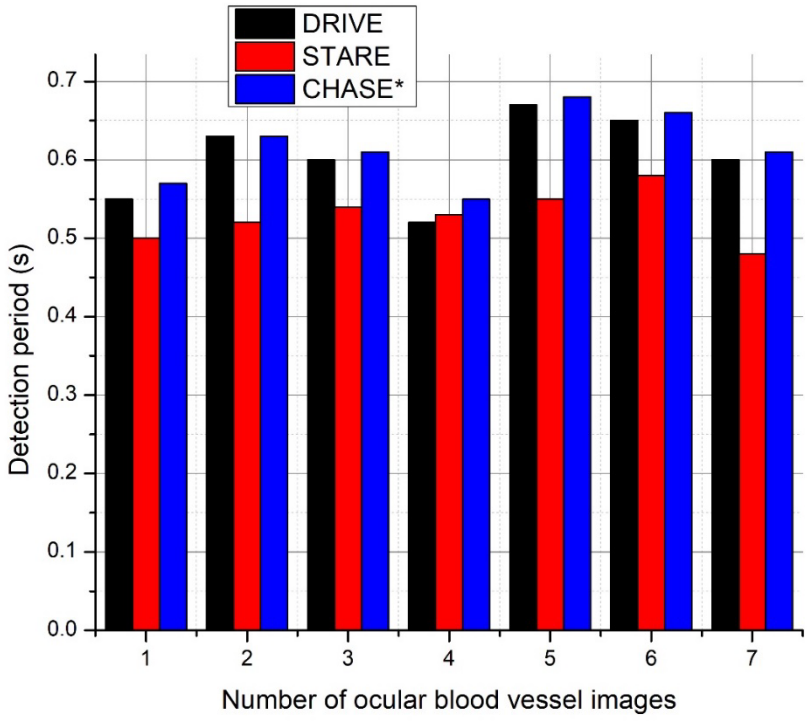

Figure 5. Detection period (s) of RU-Net segmentation process using a five-fold cross-verification technique for various datasets.

portions or patches of the picture, as opposed to the whole image, is evident during the learning phase Yang et al. (2021). The individualized handling of areas enables more diversity in the data within the learning batch, mostly due to the following factors: The quantity of retinal pictures is much greater when dealing with areas, especially five times greater in our specific scenario. It is important to note that a training batch is constructed by arbitrarily selecting areas from the whole collection of accessible photos.

Employing techniques for data enhancement to every component within the batch enhances the statistical significance of the learning set more effectively when employing patches. This mitigates the issue of excessive fitting and enhances the network's ability to generalize effectively. Both factors support network integration since a wider range of data leads to a loss function interface more closely aligned with the actual one Soomro et al. (2019). Additionally, a probabilistic map is created for each pixel in the input region, indicating the likelihood of it contributing to the BVs. The likelihood of a picture is generated by coupling the sigmoid function to the network output Tamim et al. (2020). The ultimate categorization of each pixel into one of the two categories of the issue, namely whether it is a BV pixel or not, will be decided by the threshold value used to convert the likelihood map into a binary representation.

3.1 Learning Phase

This section covers several issues related to network learning, including the selection of training picture sets for each evaluation scenario, the necessary information sources, the creation of learning data, and the loss model and variables utilized in the training procedure.

3.1.1 Collections of learning pictures: In this work, it has been chosen to use a cross-dataset learning and evaluation approach to develop the network and assess the categorizations it produces on the images from every file (DRIVE, STARE and CHASE). This is because the DRIVE, STARE and CHASE datasets do not have separate sets of learning and validation images. The network learning process involves processing a distinct collection of pictures based on the assessment dataset.

3.1.2 Origin of data: The network learning method utilizes the following details: • The original retinal image (I) refers to an RGB fundus image from which the network input regions have been derived.

Segmented image ($Segm$): The $Segm$ is a binary picture that precisely identifies the location of each pixel inside the BV. This picture has been created by experts by hand and is regarded as the definitive reference in the procedure.

The Distance Matrix to the BV Structure (DMBV) is a matrix that measures the separation between every pixel in image Im and the neighboring pixel in the BV. For every location (i,j), it holds the specific distance between the pixel (i,j) and the closest pixel in the BV (Segm):

$$DMBV_{Im}(i,j) = \min\{\|(i,j)-(u,v)\|_1 . Segm(u,v) = 1\} \quad (1)$$

Fig. 2 illustrates an instance of $Im, Segm,$ and $DMBV_{Im}(i,j)$. The picture representing the DMI matrix has been generated by proportionally scaling its values to correspond to the lowest and greatest distances with the values of 0 and 255, respectively.

Fig. 2 exemplifies the data source used during the learning stage. The picture on the left shows the initial picture, followed by the segmentation of the retinal BV and the distance image showing the proximity of each pixel to the BV.

The data ($Im, Segm,$ and $DMBV_{Im}$) has been derived from a dataset of photos in the CHASE_Db1 dataset, with a dimension of 676 × 646. The ocular circumference in these photographs is much greater than that of the DRIVE, and STARE dataset images (920 pixels compared to 526 and 646 pixels). The disparity in magnitude would compel the network during the learning stage to extrapolate the acquaintance from the input information at a significantly dissimilar scale, adversely affecting the segmentation outcomes in the trial phase. Consequently, to standardize the magnitude of all the photos used in this research and limit it to a narrower range (retinal widths ranging from 538 to 648 pixels), it has been opted to resize the images from the CHASE_Db1 dataset to the specified resolution, resulting in an ocular breadth of 652 pixels. The name assigned to this newly created dataset shall be CHASE*.

3.2 Data Enhancement

Although the learning procedure includes a minimum of 11500 data regions, the network may encounter images with lighting and color properties not included in the dataset. Only 62 or 70 photos were used to determine the learning regions. Consequently, data enhancement approaches have been used to enhance the learning set and the network's ability to evaluate photos under varying lighting and color circumstances. The augmentation of the data set occurs live throughout the learning phase, allowing for random modifications to be applied to each patch of data. These modifications include saturation changes, color changes, the addition of Gaussian noise, contrast adjustments, brightness adjustments, and horizontal or vertical inverting. These changes are applied separately and with the probability of 0.25, 0.15, 0.15, 0.3, 0.3, 0.3, and 0.3 (respectively). This ensures that about 4 out of 5 regions will get at least one alteration. Whenever a modification is made to the saturation, color, contrast, brightness, or the addition of Gaussian noise, the strength of the alteration is set arbitrarily within an area that has been experimentally established in a prior experiment. This is mostly done to guarantee that the current vascular pattern is not concealed. Indeed, the learning

dataset must include the matching patches retrieved from $Segm$, and $DMBV_{Im}$ for each modified Im patch.

3.3 Loss function

An essential step in the learning stage of a CNN is to provide a precise specification for an appropriate Loss Function (LF). The LF is a crucial factor that greatly influences the attainable outcomes of the network. Most picture segmentation issues discussed in the research are tackled using CNNs with crossover entropy as the LF. These studies mostly concentrate on creating the network design, optimizing parameters, and preliminary processing of the learning data. This work introduces a new LF in this domain that combines cross-entropy loss with its proximity to the BV. The definition of LF may be expressed as

$$LF = \sum \text{crossover entropy loss } \mathbb{C}\ DMBV_{Im} \quad (2)$$

The symbol " $\mathbb{C}$ " represents the Hadamard's element-wise matrix multiplication procedure. 12 units have increased the parameters of the distance matrix to mitigate the impact of length on the pixels close to the BV. Consequently, a mistake occurring in a pixel located 7 units away from the BV incurs a penalty that is just 1.2 times more than a mistake in a pixel neighboring the BVs, rather than 7 times greater.

4. Results and discussion

The entire process is carried out on an Intel Core i7 processor with a clock speed of 3.67 GHz, 8GB of RAM, and an NVIDIA GTX 980 GPU. The proposed approach is executed using Python 3.5.2 as the programming language, using OpenCV library 3.4 and Tensorflow framework 1.12.

A five-fold cross-verification technique has been proposed to assess the proposed method. This involves dividing the retinal pictures from every data set into five segments, allowing for five tests to be conducted for every dataset. The objective of these trials is to assess the resilience of the proposed approach. Each trial involves four segments for the learning phase and one for testing. Fig. 3 illustrates the allocation of segments for learning and testing in every trial.

Fig. 4 depicts the accuracy (%) of the RU-Net segmentation process using a five-fold cross-verification technique for various datasets. The RU-Net segmentation method has exceptional accuracy when assessed using a five-fold cross-validation approach on diverse datasets, indicating its strong resilience and dependability in segmentation tasks. In five trials, the DRIVE dataset exhibits accuracies ranging from 97.5% to 98.28%, with the third trial attaining the greatest accuracy. The modest variance in accuracy may be ascribed to disparities in the complexity or attributes of the pictures in each fold. Similarly, the STARE dataset consistently achieves high accuracy, ranging from 97.94% to 98.4%. The fifth trial achieves the maximum accuracy, indicating that RU-Net is especially competent in handling this dataset. The CHASE* dataset demonstrates outstanding performance, with accuracies beyond 98% in all trials and reaching a maximum of 99.21% in the fourth trial. The high level of precision suggests that RU-Net excels in dividing photos from the CHASE* dataset, maybe because these images possess distinct characteristics or attributes that correspond well with the model's skills. These findings highlight the usefulness of RU-Net in picture segmentation tasks on several datasets, especially demonstrating great performance on the CHASE* dataset.

Fig. 5 depicts RU-Net segmentation's detection period (s) using a five-fold cross-verification technique for various datasets. When assessed using a five-fold cross-validation approach on various datasets, the RU-Net segmentation procedure exhibits a fast and consistent detection time. Upon analyzing the detection period in seconds for different quantities of retinal pictures, we see that the duration stays consistently low and stable across all three datasets: DRIVE, STARE, and CHASE*. The detection times for the DRIVE dataset vary between 0.52 seconds and 0.67 seconds, demonstrating a high processing speed. The STARE dataset shows detection speeds ranging from 0.48 seconds, the quickest measured, to 0.58 seconds. The consistent processing speed of RU-Net highlights its effectiveness in handling these datasets. The CHASE* dataset has rapid detection times, ranging from 0.55 seconds to 0.68 seconds. The slight increase in processing time about the other datasets may be attributed to intrinsic intricacies or larger picture dimensions inside the CHASE* dataset.

The accuracy achieved is 98.28%, 98.25%, and 99.12% for the DRIVE, STARE, and CHASE* datasets, respectively, for trail 3. The mean detection period per retinal image is 0.6s, 0.53s, and 0.62s on GPU NVIDIA GTX 980 systems for DRIVE, STARE, and CHASE* datasets. Across all datasets, the RU-Net segmentation technique demonstrates remarkable speed and efficiency, with detection times consistently below one second per image. The rapid processing capability is essential in medical imaging applications, where timely efficiency is key for early diagnosis and treatment planning.

5. Conclusion

The approach entails using a CNN constructed based on a modified version of DL architecture known as RU-Net structure. The revised version features RB and BN at every level of scaling up and down. The network is supplied with regions obtained from the original picture as input and trained using a novel LF that considers the closeness between each pixel and the vessel tree. The model's output yields the probability of each pixel inside the input area being a component of the BV structure. Using the network on the segmented areas of a retinal picture makes it feasible to get a detailed mapping of the whole image, indicating the probability of

each pixel. The probability distribution map is transformed into a binary representation by applying a certain threshold. The algorithm creates the arterial segmentation. The proposed methodology is assessed on the DRIVE, STARE, and CHASE* datasets, showcasing a better equilibrium between the detection level of retinal BVs and the time needed for identification. The accuracy attained for trial 3 is 98.28%, 98.25%, and 99.12% for the DRIVE, STARE, and CHASE* datasets. The average detection time per retinal picture is 0.6 seconds, 0.53 seconds, and 0.62 seconds on GPU NVIDIA GTX 980 systems for the DRIVE, STARE, and CHASE* datasets.

Author contribution

F.R., A.M., S.S.D. wrote, reviewed and edited the article. All authors read and approved for publication.

Acknowledgment

The authors are grateful to the Kalinga University to support their study.

Competing financial interests

The authors have no conflict of interest.

References

Balasubramanian, K., & Ananthamoorthy, N. P. (2021). Robust retinal blood vessel segmentation using convolutional neural network and support vector machine. Journal of Ambient Intelligence and Humanized Computing, 12, 3559-3569.
https://doi.org/10.1007/s12652-019-01559-w

Bhatia, S., Alam, S., Shuaib, M., Hameed Alhameed, M., Jeribi, F., Alsuwailem, R.I. (2022). Retinal vessel extraction via assisted multi-channel feature map and U-net. Front. Public Health. 10, 858327.
https://doi.org/10.3389/fpubh.2022.858327

Boudegga, H., Elloumi, Y., Akil, M., Bedoui, M. H., Kachouri, R., & Abdallah, A. B. (2021). Fast and efficient retinal blood vessel segmentation method based on deep learning network. Computerized Medical Imaging and Graphics, 90, 101902.
https://doi.org/10.1016/j.compmedimag.2021.101902

Boudegga, H., Elloumi, Y., Akil, M., Bedoui, M.H., Kachouri, R., Abdallah, A.B. (2021). Fast and efficient retinal blood vessel segmentation method based on deep learning network. Comput Med Imaging Graph. 90, 101902.
https://doi.org/10.1016/j.compmedimag.2021.101902

Dang, V. N., Galati, F., Cortese, R., Di Giacomo, G., Marconetto, V., Mathur, P., ... & Zuluaga, M. A. (2022). Vessel-CAPTCHA: an efficient learning framework for vessel annotation and segmentation. Medical Image Analysis, 75, 102263.
https://doi.org/10.1016/j.media.2021.102263

Dang, V.N., Galati, F., Cortese, R., Di Giacomo, G., Marconetto, V., Mathur, P., Zuluaga, M.A. (2022). Vessel-CAPTCHA: an efficient learning framework for vessel annotation and segmentation. Med. Image Anal. 75, 102263.
https://doi.org/10.1016/j.media.2021.102263

Gegundez-Arias, M.E., Marin-Santos, D., Perez-Borrero, I., Vasallo-Vazquez, M.J. (2021). A new deep learning method for blood vessel segmentation in retinal images based on convolutional kernels and modified U-Net model. Comput. Methods Programs Biomed. Update. 205, 106081.
https://doi.org/10.1016/j.cmpb.2021.106081

Imran, A., Li, J., Pei, Y., Yang, J.J., Wang, Q. (2019). Comparative analysis of vessel segmentation techniques in retinal images. IEEE Access, 7, 114862-114887.
https://doi.org/10.1109/ACCESS.2019.2935912

Islam, M. T., Mashfu, S. T., Faisal, A., Siam, S. C., Naheen, I. T., & Khan, R. (2021). Deep learning-based glaucoma detection with cropped optic cup and disc and blood vessel segmentation. IEEE Access, 10, 2828-2841.
https://doi.org/10.1109/ACCESS.2021.3139160

Islam, M.T., Mashfu, S.T., Faisal, A., Siam, S.C., Naheen, I.T., Khan, R. (2021). Deep learning-based glaucoma detection with cropped optic cup and disc and blood vessel segmentation. IEEE Access, 10, 2828-2841.
https://doi.org/10.1109/ACCESS.2021.3139160

Jiang, Y., Zhang, H., Tan, N., Chen, L. (2019). Automatic retinal blood vessel segmentation based on fully convolutional neural networks. sym. 11(9), 1112.
https://doi.org/10.3390/sym11091112

Kim, Y.J., Walsh, A.W., Gruessner, R.W. (2023). retinopathy. Transplantation of the Pancreas, 845-857.
https://doi.org/10.1007/978-3-031-20999-4_60

Krestanova, A., Kubicek, J., Penhaker, M., Timkovic, J. (2020). Premature infant blood vessel segmentation of retinal images based on hybrid method for the determination of tortuosity. Lékař a technika-Clinician and Technology, 50(2), 49-57.
https://doi.org/10.14311/CTJ.2020.2.02

Kumar, K.S., Singh, N.P. (2023). Retinal disease prediction through blood vessel segmentation and classification using ensemble-based deep learning approaches. Neural. Comput. Appl. 35(17), 12495-12511.
https://doi.org/10.1007/s00521-023-08402-6

Moccia, S., De Momi, E., El Hadji, S., & Mattos, L. S. (2018). Blood vessel segmentation algorithms-review of methods, datasets and evaluation metrics. Computer methods and programs in biomedicine, 158, 71-91.
https://doi.org/10.1016/j.cmpb.2018.02.001

Mookiah, M. R. K., Hogg, S., MacGillivray, T. J., Prathiba, V., Pradeepa, R., Mohan, V., ... & Trucco, E. (2021). A review of machine learning methods for retinal blood vessel segmentation and artery/vein classification. Medical Image Analysis, 68, 101905.
https://doi.org/10.1016/j.media.2020.101905

Naramala, V.R., Kumar, B.A., Rao, V.S., Mishra, A., Hannan, S.A., El-Ebiary, Y.A.B., Manikandan, R. (2023). Enhancing Diabetic Retinopathy Detection Through Machine Learning with Restricted Boltzmann Machines. Int J Adv Comput Sci Appl. 14(9).
https://doi.org/10.14569/IJACSA.2023.0140961

Rutba-Aman, Rahnuma Tasmin et al. (2023). Unveiling the Veiled: Leveraging Deep Learning and Network Analysis for De-Anonymization in Social Networks, Journal of Primeasia, 4(1), 1-6, 40042

Samuel, P. M., & Veeramalai, T. (2021). VSSC Net: vessel specific skip chain convolutional network for blood vessel segmentation. Computer methods and programs in biomedicine, 198, 105769.
https://doi.org/10.1016/j.cmpb.2020.105769

Siddiqi, M.H., Salamah Alhwaiti, Y., Alrashdi, I., Ali, A., Faisal, M. (2021). Segmentation and classification of heart angiographic images using machine learning techniques. J. Healthc. Eng. 2021.
https://doi.org/10.1155/2021/6666458

Soomro, T. A., Afifi, A. J., Zheng, L., Soomro, S., Gao, J., Hellwich, O., & Paul, M. (2019). Deep learning models for retinal blood vessels segmentation: a review. IEEE Access, 7, 71696-71717.
https://doi.org/10.1109/ACCESS.2019.2920616

Tamim, N., Elshrkawey, M., Abdel Azim, G., & Nassar, H. (2020). Retinal blood vessel segmentation using hybrid features and multi-layer perceptron neural networks. Symmetry, 12(6), 894.
https://doi.org/10.3390/sym12060894

Tanvir Anjum Labir, Poly Rani Ghosh et al. (2023). Enhancing Emotion Recognition through Deep Learning and Brain-Computer Interface Technology, Journal of Primeasia, 4(1), 1-6, 40046

Triwijoyo, B.K., Sabarguna, B.S., Budiharto, W., Abdurachman, E. (2020). Deep learning approach for classification of eye diseases based on color fundus images. In Diabetes and fundus OCT. 25-57. Elsevier.
https://doi.org/10.1016/B978-0-12-817440-1.00002-4

Yang, L., Wang, H., Zeng, Q., Liu, Y., & Bian, G. (2021). A hybrid deep segmentation network for fundus vessels via deep-learning framework. Neurocomputing, 448, 168-178.
https://doi.org/10.1016/j.neucom.2021.03.085

Zhao, F., Chen, Y., Hou, Y., & He, X. (2019). Segmentation of blood vessels using rule-based and machine-learning-based methods: a review. Multimedia Systems, 25, 109-118.
https://doi.org/10.1007/s00530-017-0580-7

Zhao, F., Chen, Y., Hou, Y., He, X. (2019). Segmentation of blood vessels using rule-based and machine-learning-based methods: a review. Multimed. Syst. 25, 109-118.
https://doi.org/10.1007/s00530-017-0580-7

Zhou, S.K., Greenspan, H., Davatzikos, C., Duncan, J.S., Van Ginneken, B., Madabhushi, A., Summers, R.M. (2021). A review of deep learning in medical imaging: Imaging traits, technology trends, case studies with progress highlights, and future promises. Proc. IEEE, 109(5), 820-838.
https://doi.org/10.1109/JPROC.2021.3054390